PERGAMON

International Journal of Heat and Mass Transfer 44 (2001) 3103–3109

International Journal of HEAT and MASS TRANSFER

www.elsevier.com/locate/ijhmt

Friction in micro-channel flows of a liquid and vapor in trapezoidal and sinusoidal grooves

Jeong-Se Suh [a], Ralph Greif [b,*], Costas P. Grigoropoulos [b]

[a] *Department of Mechanical Engineering, Gyeongsang National University, Chinju 660-701, South Korea*

[b] *Department of Mechanical Engineering, Thermal Sciences Division, University of California, Berkeley, CA 94720-1740, USA*

Received 26 May 2000; received in revised form 18 October 2000

Abstract

The flow of liquid and vapor is investigated in trapezoidal and sinusoidal grooves. The effect of variable shear stress along the interface of the liquid and vapor is studied for both co-current and counter-current flows. Velocity contours and results for the friction are obtained for both trapezoidal and sinusoidal grooves. An approximate relation that was previously utilized for the friction for the liquid was modified to obtain an accurate agreement with the results for trapezoidal and sinusoidal grooves.

1. Introduction

Micro-channels with grooves have been utilized in many cooling applications to enhance heat transfer and achieve thermal control. To meet the demands of transferring increasingly larger heat fluxes, studies of the flow and heat transfer in micro-channels have been carried out to determine the capability of these systems. An early work by Ayyaswamy et al. [1] studied the capillary flow in a triangular groove. The authors studied two-dimensional, steady laminar flow with a shear free interface and obtained a solution by using the Galerkin method. Xu and Carey [2] utilized the results of Ayyaswamy et al. [1] to analyze the heat transfer in a microgroove. The influence of vapor and liquid interactions in microgrooves has also been studied. Several studies have assumed the shear stress at the liquid–vapor interface to be uniform [3–7]. Ma et al. [8] included the non-uniform interfacial shear stress by assuming that the velocity of the liquid is uniform along the interface. Khrustalev and Faghri [9] investigated the influence of the vapor and liquid interaction for flow in a rectangular groove and included in a rigorous manner the local variation of the shear stress along the interface of the liquid and the vapor. The present work studies the flow of the liquid and vapor in a trapezoidal groove and also in a sinusoidal groove [6,7,10] and includes the local variation of the shear stress at the interface. The effect of the ratio of the vapor to the liquid velocities on the friction in the liquid region is investigated. Both co-current and counter-current flows of the liquid and the vapor are studied.

2. Analysis

Capillary flow of an incompressible Newtonian fluid is considered for trapezoidal and sinusoidal grooves as shown in Fig. 1. The velocity of the liquid at the interface is significantly influenced by both the magnitude and the relative direction between the liquid and vapor flows and both co-current and counter-current flows are considered. The procedure of Khrustalev and Faghri [9] is utilized in the present work which includes the assumptions of laminar fully developed velocity profiles and constant curvature of the liquid–vapor interface. The Cartesian coordinate system is used with the z-axis coincident with the apex of the flow region as shown in Fig. 1 [1,6,7]. Assuming fully developed flow,

$$\frac{\partial w_\ell}{\partial z} = 0, \quad \frac{\partial w_v}{\partial z} = 0, \tag{1}$$

* Corresponding author. Tel.: +1-510-642-6462; fax: +1-510-642-5539.

E-mail address: greif@newton.me.berkeley.edu (R. Greif).

0017-9310/01/$ - see front matter
PII: S0017-9310(00)00331-8

Nomenclature

A	cross-sectional area (m^2)
D_h	hydraulic diameter (m), $4A/P_{wet}$
f	friction factor, $(-dp/dz)D_h/(2\rho\overline{w}^2)$
H	height of channel (m)
h	height of groove (m)
L	half-width of channel (m)
l	interface length (m)
n	unit vector normal to a surface (m)
P_{wet}	wetted perimeter (m)
p	pressure (N m^{-2})
Re	Reynolds number, $\rho\overline{w}D_h/\mu$
W	groove width (m)
w	axial velocity (m s^{-1})
x, y, z	Cartesian coordinates (m).

Greek symbols

α	contact angle
μ	dynamic viscosity (Pa s)
ϕ	angle of groove wall inclined from vertical line
ρ	density (m^3 kg^{-1})
τ	shear stress (N m^{-2}), $\mu(\partial w/\partial n)$

Subscripts

b	groove base
CL	centerline
c	wetted contact point
i	interface
ℓ	liquid
max	maximum
v	vapor

Superscripts

$*$	dimensionless
$-$	average

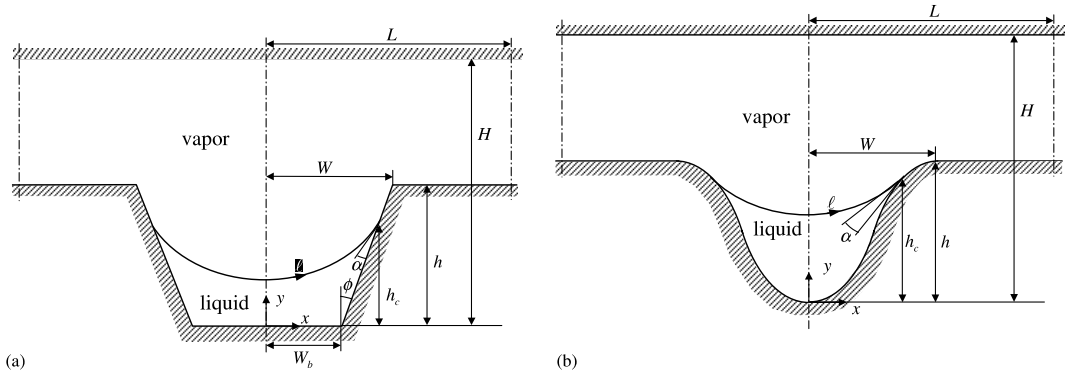

Fig. 1. Groove geometries and coordinate system: (a) trapezoidal groove; (b) sinusoidal groove.

where w_ℓ and w_v are the velocities of the liquid and vapor, respectively, in the axial direction z. The equation for the conservation of momentum reduces to

$$\frac{\partial^2 w_\ell}{\partial x^2}+\frac{\partial^2 w_\ell}{\partial y^2}=\frac{1}{\mu_\ell}\left(\frac{\partial p}{\partial z}\right)_\ell, \quad \frac{\partial^2 w_v}{\partial x^2}+\frac{\partial^2 w_v}{\partial y^2}=\frac{1}{\mu_v}\left(\frac{\partial p}{\partial z}\right)_v. \tag{2}$$

The boundary conditions for the liquid are:

$$w_\ell = 0 \quad \text{on the groove surface,} \tag{3}$$

$$\left(\mu_\ell \frac{\partial w_\ell}{\partial n}\right) = \pm\left(\mu_v \frac{\partial w_v}{\partial n}\right) \quad \text{at the interfacial surface,} \tag{4}$$

$$\frac{\partial w_\ell}{\partial x} = 0 \quad \text{at } x = 0; \tag{5}$$

for Eq. (4), the sign is positive for co-current flow of the liquid and vapor, and negative for counter-current flow. Eq. (5) is a symmetry condition. The boundary conditions for the vapor are:

$$w_v = 0 \quad \text{on the channel and groove surfaces,} \tag{6}$$

$$\frac{\partial w_v}{\partial x} = 0 \quad \text{at } x = 0 \text{ and } L, \tag{7}$$

where Eq. (7) is a symmetry condition. Since the maximum velocity of the vapor is much larger than that of the liquid at the interface, the vapor velocity at the interface is approximated to be stationary [3]:

$$w_v = 0 \quad \text{at the interface.} \tag{8}$$

The velocities and coordinates are scaled according to $h^2(-dp/dz)/\mu$ and h, respectively. Dimensionless parameters are thus introduced as

$$x^* = \frac{x}{h}, \quad y^* = \frac{y}{h}, \quad w_\ell^* = \frac{w_\ell}{h^2(-\mathrm{d}p/\mathrm{d}z)_\ell/\mu_\ell}, \quad w_v^* = \frac{w_v}{h^2(-\mathrm{d}p/\mathrm{d}z)_v/\mu_v}. \tag{9}$$

In the liquid region, the dimensionless equations for the conservation of momentum and the boundary conditions are:

$$\frac{\partial^2 w_\ell^*}{\partial x^{*2}} + \frac{\partial^2 w_\ell^*}{\partial y^{*2}} = -1, \tag{10}$$

$$w_\ell^* = 0 \quad \text{on the groove surface,} \tag{11}$$

$$\frac{\partial w_\ell^*}{\partial n^*} = \pm \frac{\partial w_v^*}{\partial n^*} \left(\frac{\overline{w}_\ell^*}{\overline{w}_v^*}\right)\left(\frac{\mu_v}{\mu_\ell}\frac{\overline{w}_v}{\overline{w}_\ell}\right) \quad \text{at the interfacial surface,} \tag{12}$$

$$\frac{\partial \overline{w}_\ell^*}{\partial x^*} = 0 \quad \text{at } x^* = 0, \tag{13}$$

where $\overline{w}_\ell$ and $\overline{w}_v$ are the average axial velocities of the liquid and vapor regions, respectively.

In the vapor region, the dimensionless equation for the conservation of momentum is

$$\frac{\partial^2 w_v^*}{\partial x^{*2}} + \frac{\partial^2 w_v^*}{\partial y^{*2}} = -1, \tag{14}$$

and the dimensionless boundary conditions are:

$$w_v^* = 0 \quad \text{at the channel and groove surfaces,} \tag{15}$$

$$w_v^* = 0 \quad \text{at the interfacial surface,} \tag{16}$$

$$\frac{\partial w_v^*}{\partial x^*} = 0 \quad \text{at } x^* = 0 \text{ and } L. \tag{17}$$

The friction factors for both the liquid and the vapor can be obtained from the following relations [8]

$$(f \cdot Re)_\ell \equiv \left(\frac{(-\mathrm{d}p/\mathrm{d}z)_\ell D_{h,\ell}}{2\rho_\ell \overline{w}_\ell^2}\right)\left(\frac{\rho \overline{w}_\ell D_{h,\ell}}{\mu_\ell}\right) = \frac{D_{h,\ell}^{*2}}{2\overline{w}_\ell^*}, \tag{18}$$

$$(f \cdot Re)_v \equiv \left(\frac{(-\mathrm{d}p/\mathrm{d}z)_v D_{h,v}}{2\rho_v \overline{w}_v^2}\right)\left(\frac{\rho \overline{w}_v D_{h,v}}{\mu_v}\right) = \frac{D_{h,v}^{*2}}{2\overline{w}_v^*}, \tag{19}$$

where $D_h = 4A/P_{wet}$ is the hydraulic diameter, and A and P_{wet} are the cross-sectional area and the wetted perimeter, respectively.

For the trapezoidal groove, the groove wall is defined by [7]

$$y^* = \begin{cases} 0 \quad (0 \leqslant x^* \leqslant W_b/h), \\ (x^* - W/h)\cot\phi, \ (W_b/h \leqslant x^* \leqslant W/h) \\ \quad \text{for } \phi < \frac{\pi}{2}, \\ 1 \quad (W/h \leqslant x^* \leqslant L/h), \end{cases} \tag{20}$$

$$x^* = \frac{W_b}{h} \quad (0 \leqslant y^* \leqslant 1) \quad \text{for } \phi = \frac{\pi}{2}. \tag{21}$$

The radius of curvature of the interface is assumed to be constant and is given by:

$$y^* = \begin{cases} \frac{h_c}{h} + \left(\frac{W_b}{h} + \frac{h_c}{h}\tan\phi\right)\tan(\alpha+\phi) \\ \quad -\sqrt{\left(\frac{W_b/h)+(h_c/h)\tan\phi}{\cos(\alpha+\phi)}\right)^2 - x^{*2}}, \quad \alpha+\phi < \frac{\pi}{2}, \\ \frac{h_c}{h}, \quad \alpha+\phi = \frac{\pi}{2}, \end{cases} \tag{22}$$

where W_b is the base width of the groove and h_c is the height of contact point of meniscus [1,6,7].

For the sinusoidal groove, the groove wall is defined by [6]

$$y^* = \begin{cases} \frac{1}{2}\left[1 - \cos\left(\frac{\pi h x^*}{W}\right)\right], & 0 \leqslant x^* < W/h, \\ 1, & W/h \leqslant x^* \leqslant L/h. \end{cases} \tag{23}$$

The radius of curvature of the interface is assumed to be constant and is given by

$$y^* = \begin{cases} \frac{W_c}{h}\left[1 + \tan(\alpha+\phi) - \cos\left(\frac{\pi W_c}{W}\right)\right] \\ \quad -\sqrt{\left(\frac{W_c/h}{\cos(\alpha+\phi)}\right)^2 - x^{*2}}, \quad \alpha+\phi < \frac{\pi}{2}, \\ \frac{h_c}{h}, \quad \alpha+\phi = \frac{\pi}{2} \end{cases} \tag{24}$$

in which $\phi = \arctan[(2W/\pi h)\mathrm{cosec}(\pi W_c/W)]$ and $W_c = (W/\pi)\arccos[1 - 2(h_c/h)]$.

3. Numerical procedure

The governing equations were solved numerically in the liquid and vapor regions, using the method of Karki and Patankar [11]. The governing equations are transformed into the curvilinear coordinate system $x = x(\xi, \eta)$ and $y = y(\xi, \eta)$ and the equations are discretized using the central difference scheme [12]. The resulting algebraic equations were solved using a non-uniform grid system with 71 nodes in the ξ direction and 25 nodes in the η direction. In the region near the surface and in the vicinity of the interface, the grids were densely distributed. Iterations were continued until changes in the velocities were less than 0.1%. It was found that the results differed by less than 0.01% from a grid system of 142×50 nodes. Calculations were also carried out for the problems studied by Ayyaswamy et al. [1] and by Ma et al. [8]. Very good agreement was obtained for the results for the friction factor for both of these studies.

4. Results and discussion

In this work results are obtained for both trapezoidal and sinusoidal grooves. Results are obtained over the range $0.5 \leqslant h_c/h \leqslant 1$, $2 \leqslant H/h \leqslant 6$, $0.3 \leqslant W/h \leqslant 0.7$,

$0 \leqslant W_b/W \leqslant 1$, $1 \leqslant L/W \leqslant 6$ and $0° \leqslant \alpha \leqslant 60°$. Note that W_b/W refers to the trapezoidal grooves.

The distributions of dimensionless velocity for the liquid flow in both the trapezoidal and sinusoidal grooves are shown in Figs. 2(a) and (b) for $h_c = 0.7h$ for co-flow and for counter-flow. Note that for counter-flow, near the interface, the negative values of the contours correspond to the liquid flow that is in the same direction of the vapor flow. Away from the interface, the liquid velocity is opposite (positive values of the contours) to the vapor flow.

The variation of the shear stress along the interface is shown in Fig. 3(a) and (b) for trapezoidal and sinusoidal grooves. The vapor flow is independent of the liquid flow since the vapor velocity is set equal to zero at the interface (Eq. (6)) and the shear stress at the interface is, therefore, solely obtained from the vapor flow. Note that when $h_c = h$, the liquid wets the entire groove. For the sinusoidal groove, when $h_c = h$, the interface is flat (yielding a rectangular vapor flow passage with slip sides) and the shear stress is constant along the interface and the bottom of the vapor channel. For the trapezoidal groove, when $h_c = h$, the magnitude of the interfacial shear stress is a maximum at the top corner of the groove. For $h_c < h$, however, the shear stress is a maximum at the centerline for both the trapezoidal and the sinusoidal grooves. This result differs from the trend presented by Khrustalev and Faghri [9] for a rectangular groove.

Results for the friction for the vapor region are shown for three cases in Figs. 4(a) and (b) in terms of the product $(f \cdot Re)_v$ for several configurations for the trapezoidal and the sinusoidal grooves. The friction-Reynolds number product, $(f \cdot Re)_v$, increases monotonically with increasing h_c. In the trapezoidal groove, the product, $(f \cdot Re)_v$, has a greater variation with respect to the wetted contact angle, α, than in the sinusoidal grooves. The results for the friction for the trapezoidal grooves can be summarized as follows:

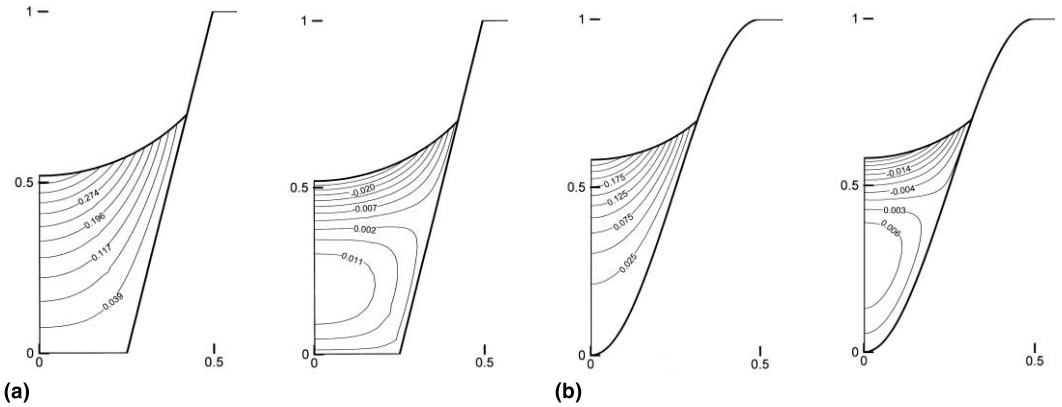

Fig. 2. Contour plots for dimensionless velocities of the liquid in co-flow (left) and counter-flow (right) for $W = 0.5h$ and $h_c = 0.7h$: (a) trapezoidal groove; (b) sinusoidal groove.

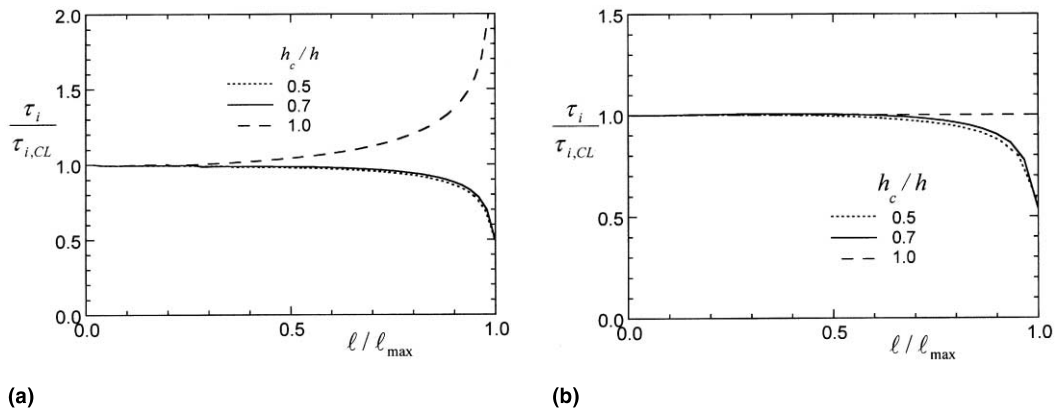

Fig. 3. The variation of dimensionless shear stress at the interface for $W = 0.5h$: (a) trapezoidal groove; (b) sinusoidal groove.

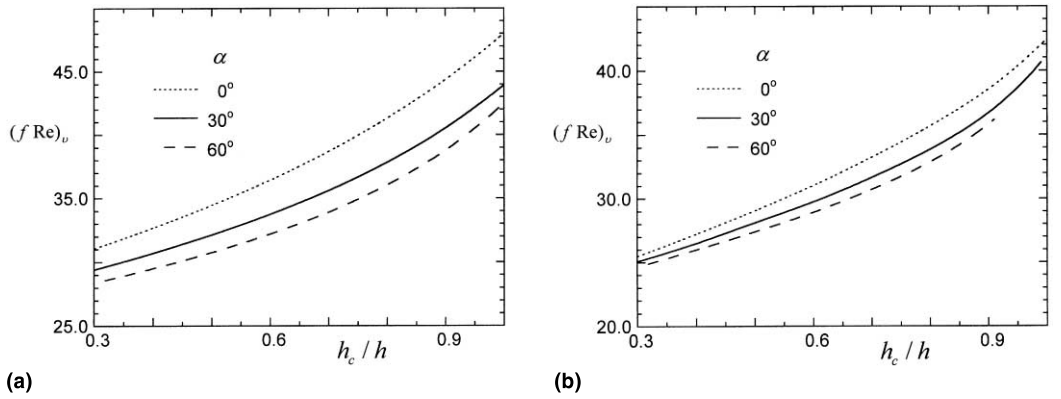

Fig. 4. Friction factor–Reynolds number product for the vapor region for three meniscus contact angles for $W = 0.5h$ and $h_c = 0.7h$: (a) trapezoidal groove; (b) sinusoidal groove.

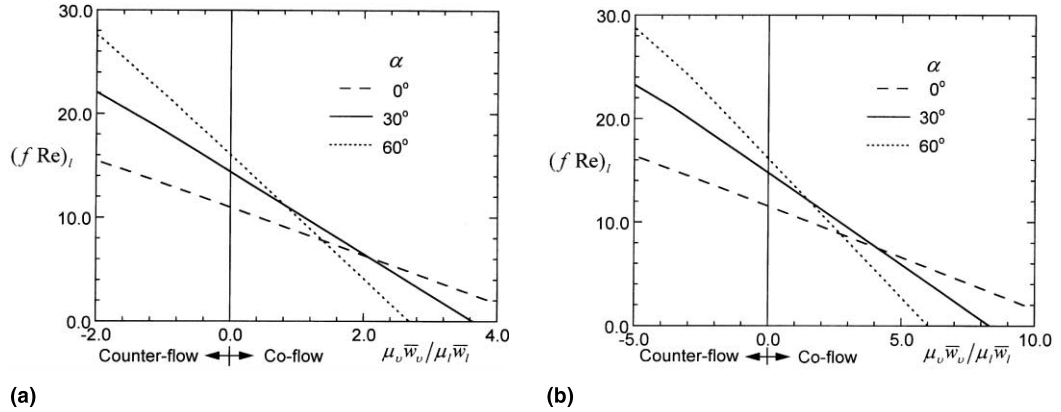

Fig. 5. Friction factor–Reynolds number product for the liquid region for three meniscus contact angles for $W = 0.5h$, $h_c = 0.7h$ and $W_b = 0.5W$: (a) trapezoidal groove; (b) sinusoidal groove.

$$(f\cdot Re)_v = \left(-0.94 + 3.8e^{\pi h_c/2h} + \frac{11.8}{1+\sin\alpha}\right) + \left(\frac{W}{L}\right)^2\left(52 + 4.6e^{\pi h_c/2h} + \frac{0.89}{1+\sin\alpha}\right), \tag{25}$$

and for the sinusoidal grooves:

$$(f\cdot Re)_v = \left(22.2 + 2.53e^{\pi h_c/2h} - \frac{4.1}{1+\sin\alpha}\right) + \left(\frac{W}{L}\right)^2\left(-29.7 + 5.43e^{\pi h_c/2h} + \frac{42.3}{1+\sin\alpha}\right). \tag{26}$$

Results for the friction for the liquid region are shown in Figs. 5(a) and (b) for several cases for the product $(f\cdot Re)_\ell$ as a function of the parameter $\mu_v\overline{w}_v/\mu_\ell\overline{w}_\ell$ for trapezoidal and sinusoidal grooves. For co-flow, the product $(f\cdot Re)_\ell$ decreases linearly as $\mu_v\overline{w}_v/\mu_\ell\overline{w}_\ell$ increases; but for counter-flow, $(f\cdot Re)_\ell$ increases almost linearly as the magnitude of $\mu_v\overline{w}_v/\mu_\ell\overline{w}_\ell$ increases. This agrees with the trend of Khrustalev and Faghri [9] for rectangular grooves. For both trapezoidal and sinusoidal grooves, for higher values of α, the product $(f\cdot Re)_\ell$ has a larger variation with $\mu_v\overline{w}_v/\mu_\ell\overline{w}_\ell$.

Schneider and DeVos [13] refer to a relation by DiCola [14] which relates $(f\cdot Re)_\ell$, for the condition with constant shear at the interface, to the friction without shear at the interface $(f\cdot Re)_{\ell 0}$ multiplied by a factor which contains a constant shear term at the interface and the groove dimensions. Schneider and DeVos [13] give approximate relations which are in good agreement with the result of DiCola [14]: [1]

$$(f\cdot Re)_\ell = (f\cdot Re)_{\ell 0}\left[1 - \frac{\tau_i^*}{3\gamma^2}\left(1 - 1.971e^{\frac{\pi\gamma}{2}}\right)\right] \quad \text{with } \gamma = h_e/W_c, \tag{27}$$

[1] For completeness, we note that Eq. (27) as presented by Schneider and Devos [13] is not valid for small values of γ.

and

$$(f \cdot Re)_{\ell 0} = \frac{8\gamma^2}{(1+\gamma)^2((1/3) - (64/\pi^5\gamma)\tan h(\pi\gamma/2))}. \tag{28}$$

Note that, for the trapezoidal groove, h_e and W_c represent the equivalent wetted depth and wetted half-width of a rectangular groove.

For the present results, $(f \cdot Re)_\ell$, with variable shear at the interface, τ_i, can be obtained from

$$(f \cdot Re)_\ell = B \cdot (f \cdot Re)_{\ell 0}\left[1 - \frac{\overline{\tau}_i^*}{3\gamma^2}\left(1 - 1.971e^{\pi\gamma/2}\right) \cdot E\right], \tag{29}$$

where

$$\overline{\tau}_i^* \equiv \frac{\overline{\tau}_i}{\mu_\ell \overline{w}_\ell / h_e} = (f \cdot Re)_v \frac{h_e}{2D_{h,v}} \frac{\mu_v \overline{w}_v}{\mu_\ell \overline{w}_\ell} \tag{30}$$

for both trapezoidal and sinusoidal grooves. Note that $\overline{\tau}_i$ denotes the average value of the variable shear stress at the interface. The functions B and E for the trapezoidal grooves are

$$B = 1.44 - \frac{0.84}{1+\sin\alpha}\left(1 - 0.19\sqrt{1 - \left(\frac{W_b}{W}\right)^2}\right), \tag{31}$$

and

$$E = -1.2 + 1.1\frac{W}{h} + 1.6e^{(W_b/W)^3} - 0.45\sqrt{\frac{W}{L}} - 1.1\alpha + \frac{h_c}{H - h_c}\left(1.6 - 0.77\frac{W}{h} - 1.6e^{(W_b/W)^3} + 1.3\alpha\right), \tag{32}$$

and for the sinusoidal grooves

$$B = 1.46 - \frac{0.67}{1+\sin\alpha}, \tag{33}$$

and

$$E = -0.15 + 0.94\frac{W}{h} - 0.13\sqrt{\frac{W}{L}} - 0.18\alpha + \frac{h_c}{H - h_c}\left(0.16 - 0.4\frac{W}{h} + 0.73\alpha\right). \tag{34}$$

We note that Eq. (29) is in agreement to within 5% of the results obtained for the full problem for the trapezoidal and the sinusoidal grooves as specified in Eqs. (10)–(17).

5. Conclusions

In this work, liquid and vapor flows have been investigated in trapezoidal and sinusoidal grooves. Both co-current and counter-current flows have been studied, and the effect of variable shear stress along the interface of the liquid and vapor is included. Correlations of the friction factors for the vapor and liquid have been obtained for both trapezoidal and sinusoidal grooves. The results show that the geometric configurations of the grooves have an important effect on the friction of the vapor and the liquid. The friction on the liquid is greatly affected by the ratio of the mean velocities of the vapor to the liquid.

Acknowledgements

This research is sponsored by DARPA MTO through the HERETIC program and SPAWAR under N66001-99-1-8914. Professor J.-S. Suh wishes to acknowledge support from the Korean Science and Engineering Foundation. We are indebted to Professor S. Thomas of Wright State University for providing us with pre-publication copies of his work. We are indebted to Professor D. Liepmann of UCB and Dr. K. Yerkes of AFRL for many helpful discussions.

References

[1] P.S. Ayyaswamy, I. Catton, D.K. Edwards, Capillary flow in triangular grooves, J. Appl. Mech. 41 (1974) 332–336.
[2] X. Xu, V.P. Carey, Film evaporation from a micro-grooved surface – an approximate heat transfer model and its comparison with experimental data, J. Thermophys. Heat Transfer 4 (4) (1990) 512–520.
[3] J.P. Longtin, B. Badran, F.M. Gerner, A one-dimensional model of a micro heat pipe during steady-state operation, J. Heat Transfer 116 (1994) 709–715.
[4] D. Khrustalev, A. Faghri, Thermal analysis of a micro heat pipe, J. Heat Transfer 116 (1994) 189–198.
[5] L. Lin, A. Faghri, Steady-state performance of a rotating miniature heat pipe, J. Thermophys. Heat Transfer 11 (4) (1997) 513–519.
[6] S.K. Thomas, R.C. Lykins, K.L. Yerkes, Fully-developed laminar flow in sinusoidal grooves, Personal communication, 2000a.
[7] S.K. Thomas, R.C. Lykins, K.L. Yerkes, Fully-developed laminar flow in trapezoidal grooves with shear stress at the liquid–vapor interface, Personal communication, 2000b.
[8] H.B Ma, G.P. Peterson, X.J. Lu, The influence of vapor–liquid interactions on the liquid pressure drop in triangular microgrooves, Int. J. Heat Mass Transfer 37 (1994) 2211–2219.
[9] D. Khrustalev, A. Faghri, Coupled liquid and vapor flow in miniature passages with micro grooves, J. Heat Transfer 121 (1999) 729–733.
[10] J. Kirshberg, D. Liepmann, K. Yerkes, Micro-cooler for chip-level temperature control, in: Proceedings of the SAE Aerospace Power System Conference, Paper No. 1999-01-1407, 1999, pp. 233–239.

[11] K.C. Karki, S.V. Patankar, Calculation procedure for viscous incompressible in complex geometries, Numer. Heat Transfer 14 (1988) 295–307.
[12] S.V. Patankar, Numerical Heat Transfer and Fluid Flow, Hemisphere, Washington, DC, 1980.
[13] G.E. Schneider, R. DeVos, Nondimensional analysis for the heat transport capability of axially-grooved heat pipes including liquid/vapor interaction, AIAA Paper No.80-0214, 1980.
[14] G. DiCola, Soluzionne analitica, amezzo della transformata di Fourier, di un problema di fusso in un canale rettangolare, Euratom C.C.R. Ispra (Italy), CETIS, 1968; cited in [13].